ATLAS New Small Wheel Phase I Upgrade: Detector and Electronics Performance Analysis

[†]Dominique Trischuk, [††]Alain Bellerive and [††]George Iakovidis
[†]*IPP CERN Summer Student*
[††]*Supervisor*

August 2016

Abstract

The High Luminosity Large Hadron Collider (HL-LHC), a planned upgrade of the LHC for 2025, will provide a challenging environment the detectors. The ATLAS muon endcap system was not designed to operate at the high rates that will be provided by the HL-LHC and must be upgraded. The New Small Wheel (NSW) will replace the current Muon Small Wheel and will provide enhanced trigger and tracking capabilities. Two new detectors, the small-strip thin gap chambers (sTGCs) and micromegas, will be installed in the NSW. The VMM chip is a custom applied specific integrated circuit (ASIC), designed at Brookhaven National Laboratory, that will serve as the frontend ASIC for the detectors in the NSW. In order to provide precise timing measurements, the VMM chip must be calibrated. This report will describe the calibration method of the electronics, in addition to energy resolution measurements for the micromegas and a charge distribution analysis of the sTGCs.

1. Introduction

LHC and HL-LHC

The LHC at CERN is the world's largest particle accelerator and collider. Consisting of two superconducting rings, the LHC is designed to collide *p-p* beams with a centre of mass energy $\sqrt{s}$ = 14 TeV and a nominal luminosity $\mathcal{L} = 10^{34}$ cm^{-2}s^{-1}. It is installed in a 27km long tunnel under the countryside surrounding Geneva, Switzerland. The goal of the LHC is to perform precise measurements of the Standard Model, which is currently the best known model of fundamental particles and their interactions. However, experimental evidence suggests that the Standard Model is incomplete. The theory does not explain dark matter or dark energy, which is approximately 95% of the universe. Nor does it explain why gravity is so weak compared the other fundamental forces. Therefore, the LHC is also looking for new observations that are inconsistent with the Standard Model, which might give us insight into where to search for new physics that can fully describe the nature of our universe.

In order to extend the reach of the physics program at the LHC, the accelerator will be upgraded in several phases. The first shutdown in 2013-2014 increased the centre of mass energy from $\sqrt{s}$ = 8 TeV to it's intended design energy of $\sqrt{s}$ = 14 TeV. In 2019, the accelerator will be upgraded again (Phase I), this time to increase the luminosity of the experiment to $\mathcal{L}$ = 2-3×10^{34} cm^{-2}s^{-1}. However, in order to push the physics even further, the HL-LHC upgrade is planned for 2025 (Phase II). This upgrade hopes to achieve 5-7 times the nominal luminosity.

ATLAS and the NSW Upgrade

The ATLAS detector is one of two general purpose detectors on the LHC ring and was designed to discover the Higgs boson, as well as perform beyond the Standard Model

searches, such as SUSY and high mass searches. However, in order to take full advantage of the HL-LHC upgrade in 2025, ATLAS must be upgraded following the same schedule as the LHC. In particular, the HL-LHC will provide ATLAS with a larger number of interaction points per bunch crossing. Thus, it is critical that ATLAS is able to operate in this high background environment (see fig.1).

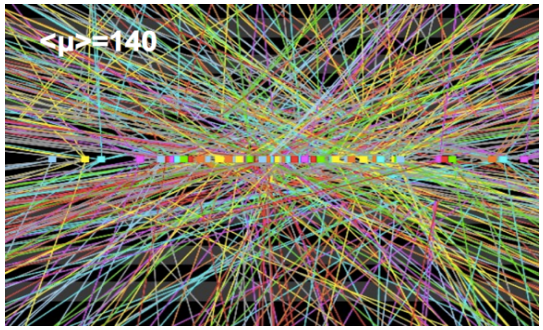

Figure 1: Simulated pile-up of the HL-LHC with an average number of interaction vertices <μ> = 140, [< μ > =(luminosity × inelastic total cross section)/ (number of colliding bunches × revolution frequency)].

The Phase I upgrade of ATLAS will focus on the calorimeter and muon Level-1 trigger systems. A 2012 analysis[1] of the data suggests that 90% of Level-1 muon triggers in the end-cap region $1.0 < |\eta^1| < 2.7$ are fake (see fig.2).

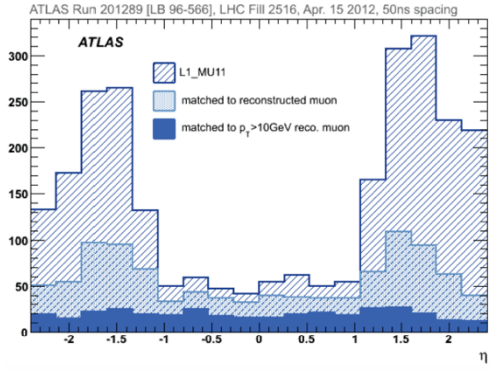

Figure 2: The η distribution of the Level-1 trigger rate. The dashed distribution is the trigger rate of the muon signals, while the light blue are the triggers that matched with muons in the inner detector. The solid blue distribution shows reconstructed muons with p_T larger than 10 GeV.

Therefore, once the luminosity is increased, ATLAS will require detectors with enhanced trigger capabilities to collect interesting events.

The New Small Wheel (NSW) is the planned upgrade of the muon spectrometer and is designed to improve tracking performance, as well as reduce the trigger fake-rate. The NSW detector components will consist of two complimentary and redundant technologies: Small-strip Thin Gap Chambers (sTGC) and MICRO MEsh GAseous Structures chambers (micromegas). Both technologies are gas detectors and will provide triggers and precise tracking data for ATLAS.

2. Micromegas

Micromegas, unlike other gas detectors, need only one amplification gap to achieve a high gain ~10^4. The detector is filled with a gas mixture of Ar+7%CO_2 and when a particle passes through the detector it ionizes these gas molecules in the drift gap. An electric field is applied across the drift gap so that the electrons created during ionization drift towards the cathode and the amplification gap. Once the electrons pass through the micromesh they create an avalanche in the amplification gap, this signal can then be read out by the strips. Figure 3 shows a side view of the micromegas detector.

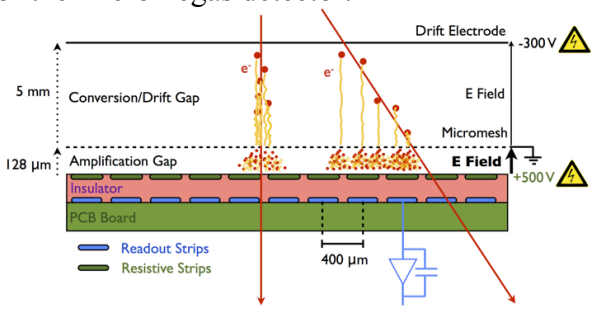

Figure 3: Side view of the micromegas showing a particle passing through the detector ionizing the gas and the electrons avalanching in the amplification gap.

[1] The pseudorapidity η is defined by the polar angle θ as $\eta = -\ln(\tan(\frac{\theta}{2}))$, where the z, x and y axes point from the interaction point along the beam, towards the centre of the LHC ring and upwards respectively.

3. Small-strip Thin Gap Chambers

The sTGCs are gas detectors based on proven TGC technology. In order to provide fast triggers, pads have been added to the sTGCs for muon track identification and readout region definition. Under the pads are wires and strips, which will be used for tracking muons. A resistive carbon layer is also added between the wires and strips to protect the readout elements against discharge. Similar to the micromegas, the sTGCs have an electric field across the gap and are filled with a gas mixture (n-pentane+55%CO_2) to create primary ionization electrons, which drift and amplify, before being detected on the readout elements. Figure 4 shows a side view of the sTCGs.

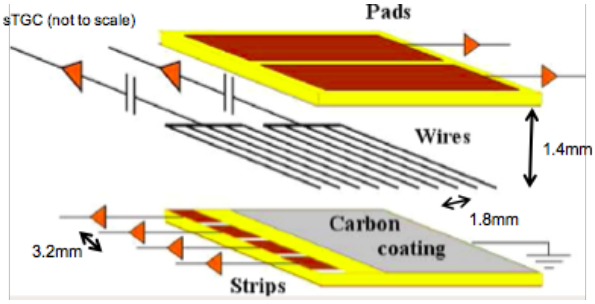

Figure 4: A side view of the sTGCs, showing the three layers: pads, wires and strips.

4. VMM Timing Calibration

NSW Electronics

The electronics system of the NSW consists of custom ASICs and various networks, which includes on-detector and off-detector elements. The VMM chips are custom ASICs that will serve as the frontend ASIC for both the sTGCs and the micromegas. Each VMM chip has 64 channels that are connected to the detector readout elements – strips (sTGC & MM), pads (sTGC) and wires (sTGC). Since the VMMs are linear electronics, the Analog to Digital Convertor (ADC) counts of the chip are linearly proportional to the charge (in pC) and timing (in ns) of the collected muon tracks. Therefore, when a particle passes through the detector it can be determined precisely when and how much charge the particle deposited on its way through the detector.

Method

The VMMs measure time by a Time Detector (TD), which is then digitized by an 8-bit ADC once the pulse peak is detected. This creates a ramp slope, which may vary from channel to channel. Therefore, it is essential to perform an accurate calibration in order to achieve precise timing measurement. During calibration, a pulse generator is used to inject charge at time t_A and the Time to Amplitude Convertor (TAC) ramp is forced to be read out at a fixed time t_{CS}, which is determined by an external clock. The Time Detector Output (TDO) is the amplitude of the TAC ramp and is a measurement of the timing of an event. Figure 5 shows the time calibration method.

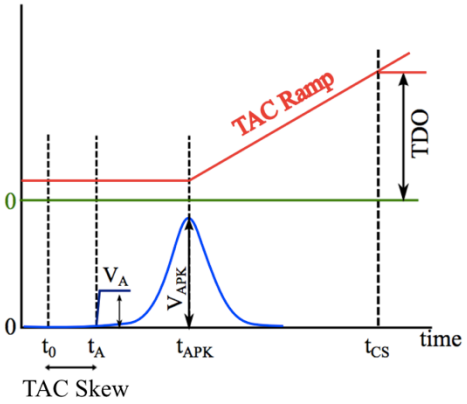

Figure 5: TDO measurement diagram.

The time at which the pulse is injected is skewed in 3.125 ns increments. In other words, the time difference between t_A and t_0, called the TAC skew, increases. This means the peak of the ADC pulse falls closer to t_{CS}, resulting in a smaller TDO. Performing a linear polynomial fit of the TDO vs. TAC

skew creates a calibration line that relates any TDO count to time in ns.

Data Analysis

Using this method, calibration fits can be plotted for each channel in the VMM. These fits determine a TAC slope and TDO offset (intercept) specific to a given channel in the chip. These values are used to calibrate the timing information from the VMMs (see fig.6).

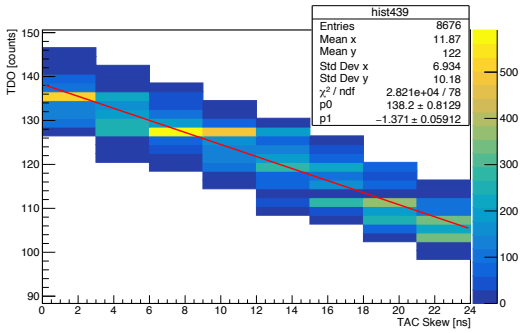

Figure 6: A time calibration plot showing the relationship between ADC counts and ns for one channel of the VMM chip. The linear fit of the data is shown in red.

Figure 7 shows how the TAC slope and TDO offset values vary across the 64 channels of one VMM chip.

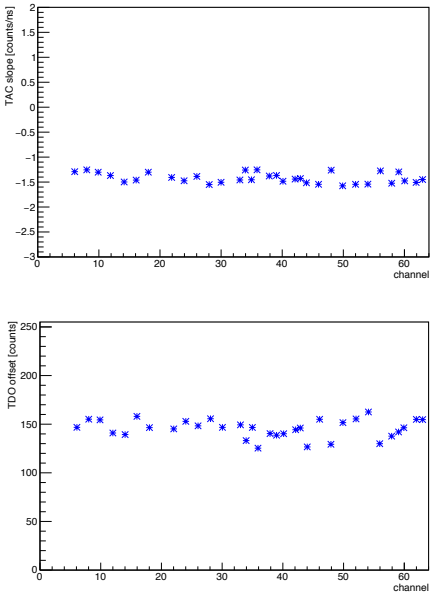

*Figure 7: **Top**: Channel distribution of the TAC slope for a VMM chip after a calibration run. **Bottom**: TDO offset for the same VMM chip*

These plots can be used to evaluate the performance of the chip. In an ideal world these values would be constant across the channels and no calibration would be needed.

However, it was observed that some channels had malfunctions during the calibration runs. In some cases, the VMM chips would produce high TDO counts for high TAC skew times. This signature is shown below in figure 8.

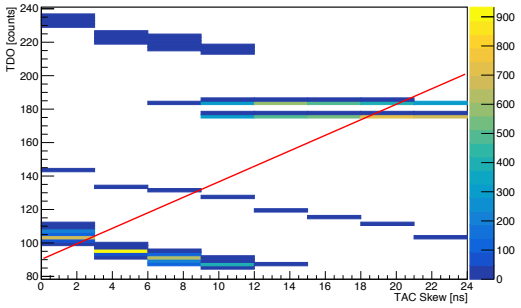

Figure 8: Calibration run with high TDO counts for large TAC skew. The linear fit of the data is shown in red with a positive slope

The linear fit of a distribution gives a positive slope, which is not consistent with the calibration method. An increasing TAC skew should *decrease* the TDO count. More work is still needed to understand why this signature occurs and what can be done to correct for this effect during calibration runs. Nevertheless, applying a sophisticated cut, which takes into account the initial TDO distribution of the first TAC skew, allows the effect from the malfunctions to be excluded from the linear fit (see fig.9).

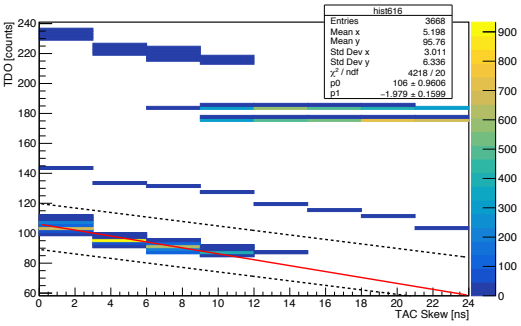

Figure 9: Calibration plot for the same channel in figure 8. Now the fit is only applied only to data between the two dashed lines.

Using this cut method, even channels with this type of malfunction can be calibrated. Moreover, this method can also be used to remove noise that may be present during calibration runs.

5. Energy Resolution

The energy resolution of a gas detector is a characteristic of the chamber that can be measured using the energy spectrum. The energy resolution can be used to help understand the gain of the detector. However, this paper will only discuss the energy resolution measurements of the micromegas.

Measurement Method

To measure the energy spectrum of the micromegas, the detector was first filled with the Ar+7%CO_2 gas mixture. A specialized counter (MCA counter) was connected to the readout elements and the counter was set to trigger on the micromesh. An iron 55 (^{55}Fe) source was placed on top of the detector to provide a constant signal. The set up of the experiment is shown in figure 10.

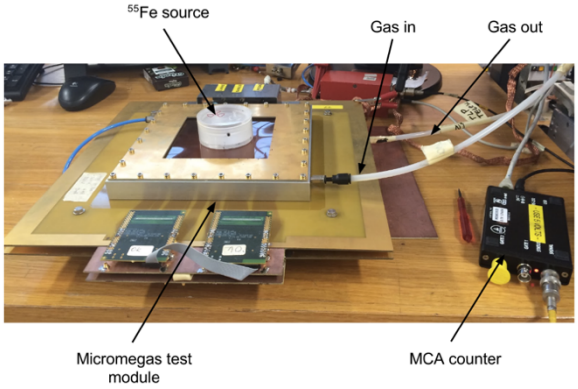

Figure 10: A micromegas test module set up for energy resolution measurements.

It is useful to use an ^{55}Fe source since it has a well known energy spectrum. The main emission line of ^{55}Fe is at 5.9 keV. However, in some cases electrons are emitted from the K-shell of the argon molecules present in the gas mixture. This effect produces a secondary peak at 2.9keV in the iron spectrum, called the argon (Ar) escape peak.

Changing the amount of applied voltage to the detector changes the shape and position of the two peaks in the iron spectrum. Measuring the relative distance between the peaks, as well as their size and shape, provides information about the characteristics of the detector. In particular, the energy resolution of the detector is calculated as follows:

$$E_{res} = \frac{FWHM}{mean} \times 100\% \quad (1)$$

where FWHM is the full width half max of the iron peak and mean refers to the mean of the same peak.

For this experiment, the energy spectrum at V=530V, V=540V and V=550V were measured and the energy resolution was calculated with a Gaussian fit of the distribution.

Results

Figure 11 shows the iron spectrum for an applied voltage of 550V, which gave the highest energy resolution of 23.93%. The applied voltages of 530V and 540V gave energy resolutions of 24.63% and 26.94% respectively.

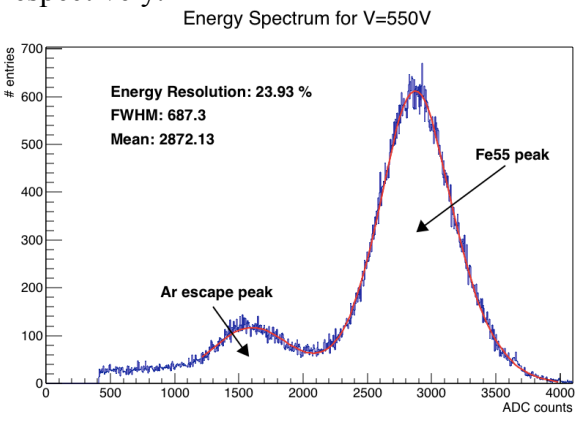

Figure 11: The energy spectrum for micromegas with an applied voltage of 550V. The blue distribution shows the data collected from the MCA counter, while the red line is the Gaussian fit. The ^{55}Fe and Ar escape peak are shown on the plot, as well as the energy resolution of 23.93%.

6. sTGC PDO Analysis

FNAL Test Beam 2014

In 2014, a sTGC quadruplet was tested in at the Fermilab National Accelerator Laboratory (FNAL). The sTCG quadruplet was placed perpendicular to the beam, along with pixel layers that gave the position of the beam in the y direction. Figure 12 shows a schematic and a picture of the test beam setup. The data from this test beam was saved in root files and used for the following analysis.

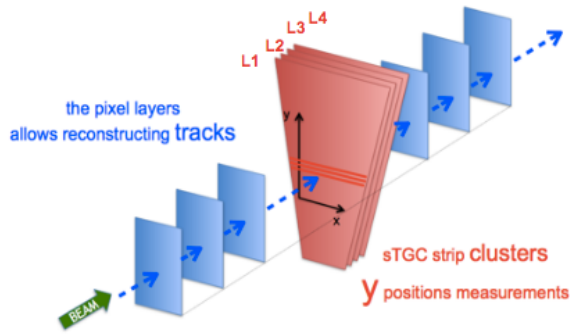

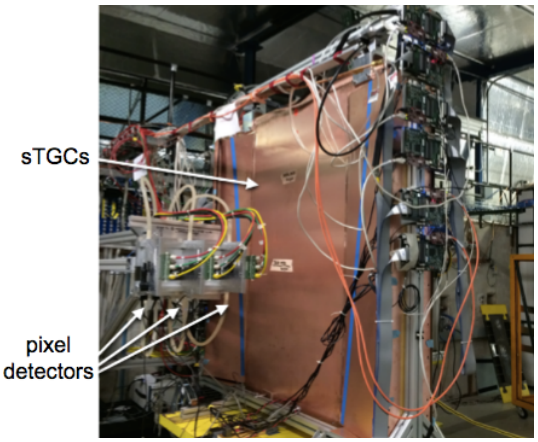

Figure 12: ***Top:*** *A schematic of the FNAL test beam setup showing the four layers of the sTCG quadruplet and the pixel telescope.* ***Bottom:*** *A picture from the FNAL test beam showing the same setup as the schematic above.*

PDO Analysis

The VMM chips also readout charge information from the detector elements in term of a Peak Detector Output (PDO). The PDO is defined as the maximum of the ADC pulse shown in figure 5. Due to the linearity of the VMM, the PDO of each channel is proportional to a charge in pC and thus is an estimator of the charge collected. Looking at the PDO distribution across the strips of the sTGCs shows the charge distribution created by the particle on it's way through the detector. Since the location of the track was known in this test beam (due to the tracking pixel layers) normalizing and centering the PDO distribution about the track position provides an estimator of the average charge distribution for all the events.

Results

The normalized and centred PDO distribution for each layer for one run is plotted below in figure 13. The x-axis is in units of strip pitch, which is defined as the distance between the centre of two adjacent strips. The zero of the x-axis is the position of the track as defined by the pixel detectors.

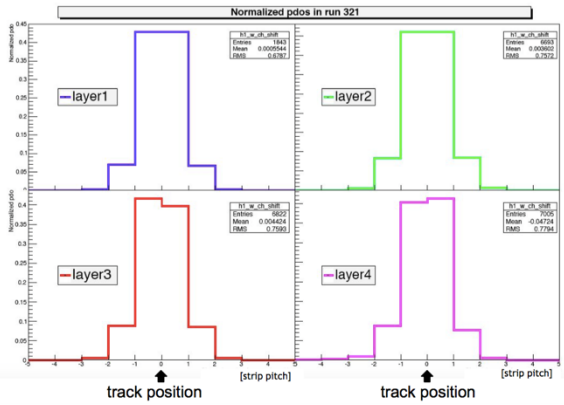

Figure 13: The normalized PDO distributions for each layer of the sTGC quadruplet for Run321. The distribution is centred at the track position.

The results show that the average charge distribution is fairly symmetric about the track position and each layer is similar in shape. To illustrate this more clearly, the following plot (fig.14) shows the four layers overlapped, as well as the average distribution across the four layers.

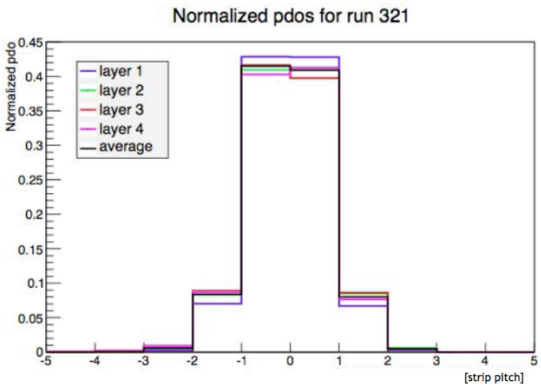

Figure 14: The PDO distributions of the four layers overlapped with a calculated average plotted in black.

In the future this PDO charge distribution analysis can be used to compare average charge distribution to detector simulations to help evaluate the detector's performance.

7. Conclusion

In summary, the current Muon Small Wheel in ATLAS cannot handle the trigger rates that the LHC luminosity upgrades will provide and thus needs to be upgraded in order to take full advantage of the HL-LHC. Two new detector technologies will be installed in the NSW to provide fast triggers and precise particle tracking.

The VMM chips will be used as the front ASICs for both detectors and require calibration in order to give precise timing measurements. A cut method has been described in this paper that will allow channels with data collection malfunctions to be calibrated.

In addition, an energy resolution measurement for the micromegas was done at three different applied voltages (530V, 540V, 550V). The highest energy resolution of 23.93% was found at 550V.

Finally, a PDO distribution analysis of the 2014 FNAL test beam was performed to provide an estimate for the average charge distribution for the sTGCs. These results can be used in the future for detector performance analysis.

---

[1] ATLAS New Small Wheel Technical Design Report, CERN-LHCC-2013-006, June, 2013

[2] G. Iakovidis, "Research and Development in Micromegas Detector for the ATLAS Upgrade," CERN-THESIS-2014-148, October, 2014.